ISSN: 2994- 9459

Research Article

Current Research in Statistics & Mathematics

Optimization of Hydraulic Simulation, Computational Time, and and Mesh Size of 2D and 3D Models Applied to the Main Open Channel of the Pocsi District, City of Arequipa

Ernesto Yana De La Riva[1]*, Sarahid Aleman Durand[1] and Walter Yana De La Riva[2]

[1]*Civil Engineering, Technological University of Peru, Peru*

[2]*Civil Engineering, Catholic University of Santa Maria, Peru*

***Corresponding Author**
Ernesto Yana De La Riva, Civil Engineering, Technological University of Peru, Peru.

Submitted: 2023, Oct 10; **Accepted**: 2023, Nov 03; **Published**: 2023, Nov 29

Citation: Yana, E., Aleman, S., Yana, W. (2023). Optimization of Hydraulic Simulation, Computational Time, and and Mesh Size of 2D and 3D Models Applied to the Main Open Channel of the Pocsi District, City of Arequipa. *Curr Res Stat Math, 2*(1), 77-96.

Abstract

Currently, in Peru engineering is going through a period of computer revolution, which means that knowledge related to new technologies must be constantly updated, having as tools data processing programs and software to obtain accurate results and optimize the development time of hydraulic projects. The present research determined the optimization of the computational time and mesh size of an open channel using the 2D models of Iber and 3D of Flow 3D. Therefore, the methodology of the study identified a quantitative approach, type of analytical research and experimental design. Moreover, for the development of the research, the following variables were identified: mesh size, computational time, 2D and 3D modelling. At first, the channel was sectioned into 12 sections of different roughness and then simulated with two computers of different characteristics and finally performed a comparative analysis of the models. By correlating the measurement of computational time with the level of accuracy and precision of the mesh size, an optimal model could be obtained. Finally, the hydraulic response in 2D and 3D models maintains an acceptable margin. In brief, 2D models have a shorter computational time and high performance in hydraulic structures and 3D models boast greater computational time and high impact of detail sensitivity in suggestive phenomena.

Keywords: Hydraulic simulation, Computational time, Meshing size, Iber, Flow 3D.

Abbreviations

C_i	Location of curve I, according to the corresponding section.
R_i	Location of the steep slope channel i, according to the corresponding section.
F_i	Location of the drop i, according to the corresponding section.
FR	Froude number.
Q	design flow (m3/s).
p_i	Wetted perimeter of channel control section (m).
n_0	Basic value of n for straight channels.
n_1	Value to be added to no.
n_2	Value of variation of shape and size of the cross section.
n_3	Value to consider obstructions.
n_4	Vegetation and flow conditions.
m_5	Effect by steep curves of the channel.
SNIP	Sistema administrativo peruano de proyectos de inversión pública.
S_i	Section i of the channel under study.
S_i‰	Average slope per thousand of section i.
Sbc	Type of subcritical regime.
Spc	Type of supercritical regime.
v	Flow velocity (m/s).
y	Flow depth (m).

1. Introduction

The analyzed channel is in the high Andean zone of Arequipa, Peru. Built at the request of the organization of the populated center of Pocsi, to solve the deficit of water resources for agricultural use. In this context, the purpose of this research concerns the optimization of hydraulic simulation in open channels through the use of statistical methods. That is, determine the standard deviation,

average to obtain the accuracy and precision of the three meshes used (5 cm, 10 cm and 20 cm). Then relate the data to the correlation coefficient of computational time analysis between 2D and 3D models.

Finally, it is expected to determine the shortest computational time and optimal mesh size applied to the main open channel of the Pocsi district. This channel has a length of 2,113 km and is located on the route of the Arequipa - Omate 34D highway between the reservoirs of Huicchuna, Piaca and Tucumpaya.

1. 1 Area of Study

The rural open channel of the Pocsi district is located at 16º 29' 45" south latitude: at 71º 20' 05" west longitude at 3 045 m.a.s.l., south of Peru. The predominant topography adjacent to the channel is mainly rugged, centered on slopes of evident inclination, having scarce areas of gentle topography; and it spread on the slopes of the Pichu volcano preserving a cold climate [1]. As shown in Figure 1.

	N°	Progressive	East	North	Altitude
First point	0	0+000	247060.2	8171650.2	3163.7
Last point	107	2+113	245518.8	8172739.2	3087.5

Table 1: Layout channel survey points

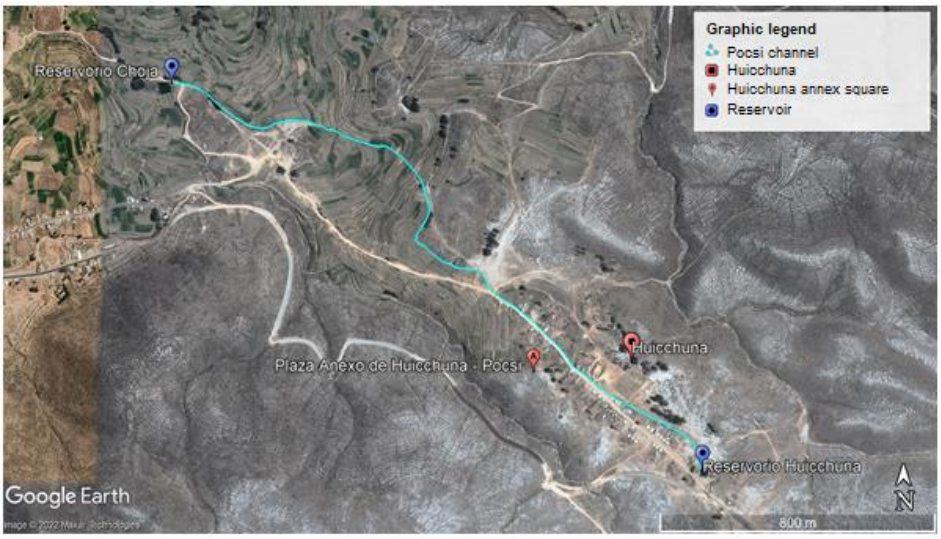

Figure 1: Area of study (Google Earth, 2021)

2. Methodology

The present research aims to detect the optimal model of hydraulic simulations in 2D and 3D models of the open channel under study. Therefore, three types of meshes (5 cm, 10 cm, and 20 cm) were adapted for each simulation. In addition, each hydraulic modelling was performed on two computers of different hardware. In order to obtain an acceptable mesh size and computational time, through a systematized procedure.

2.1 Hydraulic Models

2.1.1 Iber 2D V 2.5.2 Model

Iber's 2D hydraulic modelling is a representation of physical and numerical scenarios to realistically identify, generate, and validate possible scenarios of hydraulic problems. It supports various adaptations aimed at preventing the damage that can occur when using hydraulic structures [2].

The Iber software incorporates the Saint-Venant hydraulic mathematical model that arises from deduction following the equations of quantity of motion.

2.1.2 Forces due to Hydrostatic Pressure

According to (Ring, 2021) in a differential fluid particle, the forces due to pressure are established at the point P located in the center of the particle.

$$F_{px} = -\frac{\partial p}{\partial x}\, dxdydz \quad (1)$$

$$F_{py} = -\frac{\partial p}{\partial y}\, dxdydz \quad (2)$$

$$F_{pz} = -\frac{\partial p}{\partial z}\, dxdydz \quad (3)$$

External Forces

The main external force is due to the acceleration of gravity, that is, the own weight of the fluid, which acts in the negative direction of "z" and is obtained as:

$$W = -\rho dxdydz\, g \quad (4)$$

Forces due to Viscous Effects

The stresses act in the "x" direction of the differential fluid particle then, from Newton's second law, it follows:

$$a_x = \frac{Du}{Dt} = -\frac{1}{\rho}\frac{\partial \rho}{\partial x} + \frac{1}{\rho}\left(\frac{\partial \tau_{xx}}{\partial x} + \frac{\partial \tau_{yx}}{\partial y} + \frac{\partial \tau_{zx}}{\partial z}\right) + \underline{X} \quad (5)$$

$$a_y = \frac{Dv}{Dt} = -\frac{1}{\rho}\frac{\partial \rho}{\partial y} + \frac{1}{\rho}\left(\frac{\partial \tau_{xy}}{\partial x} + \frac{\partial \tau_{yy}}{\partial y} + \frac{\partial \tau_{zy}}{\partial z}\right) + \underline{Y} \quad (6)$$

$$a_z = \frac{Dw}{Dt} = -\frac{1}{\rho}\frac{\partial \rho}{\partial z} + \frac{1}{\rho}\left(\frac{\partial \tau_{xz}}{\partial x} + \frac{\partial \tau_{yz}}{\partial y} + \frac{\partial \tau_{zz}}{\partial z}\right) + \underline{Z} \quad (7)$$

Flow 3D Model

Flow 3D is a mathematical model whose processing includes CFD (Computational Fluid Dynamics), developed by the Santa Fe Institute, New Mexico, USA and Flow Science, Inc. The software uses a variety of numerical methods to solve the equations of characterized fluid movement.

The Flow 3D software develops the Navier-Stokes differential equations, where it incorporates the transport equations that constitute within it: the equations of conservation of mass, conservation of motion and conservation of energy.

Differential Equation Conservation of Mass

The equation of conservation of masses originates from the law of the principle of conservation of mass, it is defined as follows:

$$\frac{\partial u}{\partial x} + \frac{\partial v}{\partial y} + \frac{\partial w}{\partial z} = 0 \quad (8)$$

Momentum Conservation Equation

The conservation of motion equation is a mathematical demonstration of Newton's second law (Guncay, 2017), it is expressed as follows:

$$\rho\frac{Du}{Dt} = -\frac{\partial \rho}{\partial x} + \rho g_x + \mu\left(\frac{\partial^2 u}{\partial x^2} + \frac{\partial^2 u}{\partial y^2} + \frac{\partial^2 u}{\partial z^2}\right) \quad (9)$$

$$\rho\frac{Dv}{Dt} = -\frac{\partial \rho}{\partial y} + \rho g_y + \mu\left(\frac{\partial^2 v}{\partial x^2} + \frac{\partial^2 v}{\partial y^2} + \frac{\partial^2 v}{\partial z^2}\right) \quad (10)$$

$$\rho\frac{Dw}{Dt} = -\frac{\partial \rho}{\partial z} + \rho g_z + \mu\left(\frac{\partial^2 w}{\partial x^2} + \frac{\partial^2 w}{\partial y^2} + \frac{\partial^2 w}{\partial z^2}\right) \quad (11)$$

Energy Conservation Equation

The energy conservation equation comes from the first law of thermodynamics, represented by Fourier's law of heat transfer:

$$\rho\frac{Du}{Dt} = K\left(\frac{\partial^2 T}{\partial x^2} + \frac{\partial^2 T}{\partial y^2} + \frac{\partial^2 T}{\partial z^2}\right) - \rho\left(\frac{\partial u}{\partial x} + \frac{\partial v}{\partial y} + \frac{\partial w}{\partial z}\right) \quad (12)$$

Cowan's method

The general equation to estimate the roughness and obtain the values of n and m based on the material of the perimeter of the channel, irregularities, variation in the cross section among others (Eq. (13)).

$$n = (n_o + n_1 + n_2 + n_3 + n_4)m_5 \quad (13)$$

The constant no is the basic value of n for straight channels, n_1 is the value to be added to n_o, n_2 is the value of variation in shape and size of the cross section, n_3 is the value to consider obstructions, n_4 is the vegetation and flow condition and m_5 is the effect by sharp curve of the channel.

Horton and Einstein Method

To determine the weighted roughness, the hydraulic area is divided into various parts (A1, A2, etc.) with their corresponding wetted perimeter (p1, p2, etc.). Thus, the Horton and Einstein criterion assumes that each part of the hydraulic area has the same velocity, obtaining the following equation:

$$n = \left[\frac{\sum_{i=1}^{N} p_i {n_i}^{1.5}}{p}\right]^{2/3} \quad (14)$$

Mesh Size

According to the mesh size for the simulation was established to have varied results between the meshes and the level of accuracy - precision of the chosen software [3]. Meshes of 5 cm, 10 cm and 20 cm have been used to simulate the channel in 2D and 3D models.

Geometric Characteristics

The main channel under study is a rectangular type with the following measures: base width of 0.60 m, with a coating thickness of 0.15 m in the design according to the technical file, with a design flow of 0.2425 m^3 / s, the radio of curvatures should not fall below 1.20 m.

Georeferencing

The spatial positioning of the geographical location in the UTM coordinate system of the channel under study belongs to World Geodetic System 84 (WGS84) zone 19S. For its part, the UTM coordinates were obtained from the technical file of the public investment project (SNIP) and were corroborated in the field with a Garmin Montana GPS where 107 points were located.

Computers

For the simulation of the Iber and Flow 3D models, two computers with similar characteristics were used, as presented in Table 2, this aspect was considered to determine the type of equipment recommended for simulation with the software.

Characteristics	Computer A	Computer B
Computer Name	DESKTOP-UHOBHV0	DESKTOP-3S7IB5J
Operating system	Windows 10	Windows 10 Pro
CPU Central Unit	64 bits	64 bits
Maker	LENOVO	HP
Processor	Intel Core i7	Intel Core i7
RAM	16384 MB	16384 MB
Generation	3	10
Disk size	1.19 GB	574 MB
Video card	10183 MB	8210 MB
VRAM display memory	2017 MB	128 MB
Storage	465 GB	465 GB
Time of use	6 years	1 year

Table 2: General properties of each computer

Division of the Channel in 12 Sections

The channel was divided into 12 sections, based on the analysis of the changes of particularities in the material and conditions to characterize each section. As shown in Figure 2. Therefore, to determine the roughness values, various methods were chosen according to the characteristics of each section, including values of Ven Te Chow, Cowan's method, Horton, and Einstein method. See in Table 3.

Section	Roughness	Eq. Number
1	0.0167	Eq. (14)
2	0.0171	Eq. (14)
3	0.018	Eq. (14)
4	0.021	Eq. (13)
5	0.017	Vent Te Chow
6	0.0143	Eq. (14)
7	0.0143	Eq. (14)
8	0.014	Vent Te Chow
9	0.0143	Eq. (14)
10	0.0156	Eq. (14)
11	0.014	Vent Te Chow
12	0.014	Vent Te Chow

Table 3: Roughness assigned by section.

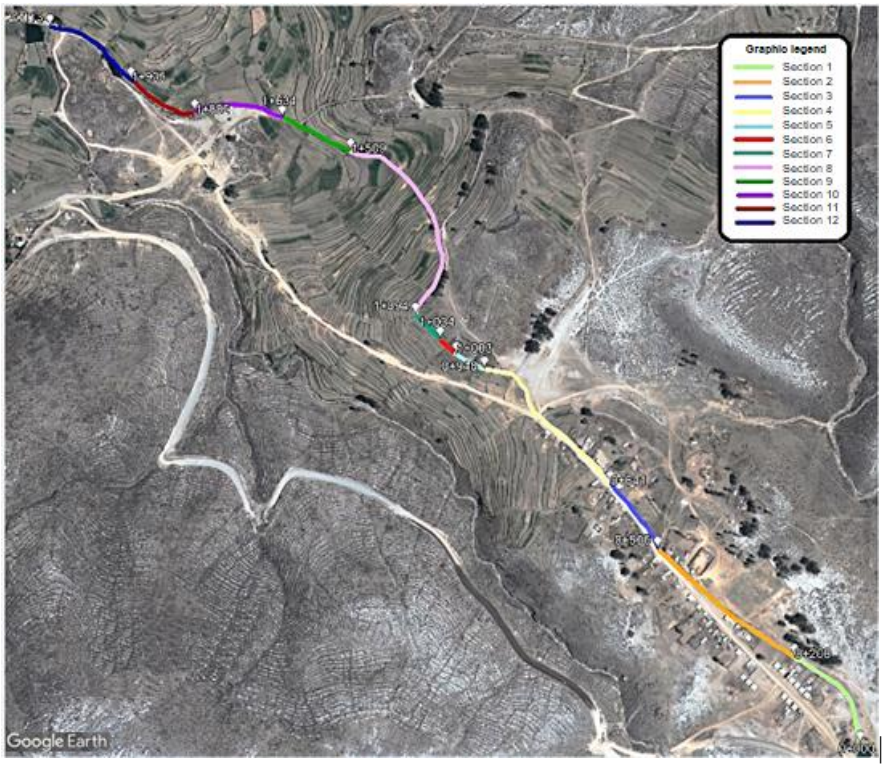

Figure 2: Division by sections of the study channel (Google Earth, 2021)

Creation of Scenarios

In the first instance, to generate the scenarios, the 12 sections in which the channel was divided, the dimensional models (2D and 3D), the 3 mesh sizes (5 cm, 10 cm and 20 cm), the two computers of different hardware and the design flow 0.2425 m3/s considered maximum capacity were taken into account. In that manner, a total of 144 scenarios were simulated. As seen in Figure 3.

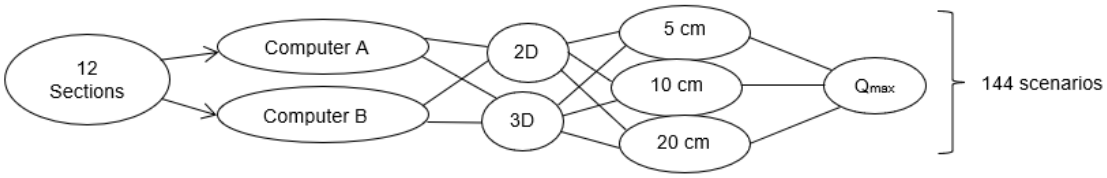

Figure 3: Creating scenarios for hydraulic simulation.

Table 4 then shows the general characteristics of the 2D and 3D models for the corresponding simulations.

Conditions	Iber	Flow 3D
Geometry	• Imported in Civil 3D .dwg format.	• Imported in Civil 3D .dwg format.
	• It is processed in format. SketchUp stl.	• It is processed in format. SketchUp stl.
	• Discretization of geometry by means of finite elements.	• Discretization of geometry by means of finite volumes.
Sections	• 12 sections were proposed according to the field inspection.	• 12 sections were proposed according to the field inspection.
Roughness	• The equations of Cowan, Horton and Einstein and theory of Vent te Chow were used.	• The equations of Cowan, Horton and Einstein and theory of Vent te Chow were used.
Mesh	• Meshing size: 5 cm, 10 cm, and 20 cm.	• Meshing size: 5 cm, 10 cm, and 20 cm.
	• Structured mesh of square elements.	• Structured mesh of cubic elements.
Boundary conditions	• Flow conditions are entered into the nodes of the mesh contour.	• Flow conditions are entered into the first mesh block.
	• Q = 0.2425 m^3/s	• Q = 0.2425 m^3/s
Turbulence model	• k - e	• RNG

Table 4: General characteristics of the models adapted from [4].

Comparison Criteria

The 2D and 3D simulation was carried out with meshes of 5 cm, 10 cm, and 20 cm. With this, the hydraulic response and computational time for each mesh are obtained. Then, we proceed to compare these variables to obtain the optimal mesh in 2D and 3D models independently.

Then, we proceed to compare 2D vs 3D models. In this case, the degree of accuracy and precision of the depth is analyzed from the hydraulic response. In the case of computational time, the average cumulative time for each mesh was determined with the corresponding correlation coefficient.

3 Results and Discussions

Hydraulic Analysis

The hydraulic flow is manifested at the rate of the criteria of time and space. The channel temporarily has a permanent flow. On the other hand, spatially is classified in varied flow, within it is divided into rapidly varied flow. However, it is also classified as gradually varied flow, since there are sections where it is evident that there is no abrupt change in the variables of the depth and velocity.

Slope Effect

The effect of slopes is the consequence of the variability of hydraulic flow. It is observed that the slope is the intermediate value between the depth and velocity since they have an inversely proportional relationship. In the longitudinal profile, Figure 4, the values of the average slopes in the sections are observed (S1‰ = 9.50, S2‰ = 6.9 0, S3‰ = 13.20, S4‰ = 14.96, S5‰ = 5.25, S6‰ = 5.70, S7‰ = 0.54, S8‰ = 79.10, S9‰ = 45.70, S10‰ = 23.50, S11‰ = 1.58 and S12‰ = 1.68). The slopes denote great variation in length. This leads to specifying that the effect of the slope generates local characteristics within the channel such as steep slope channel and drops that must adapt to the topographic environment [5-10].

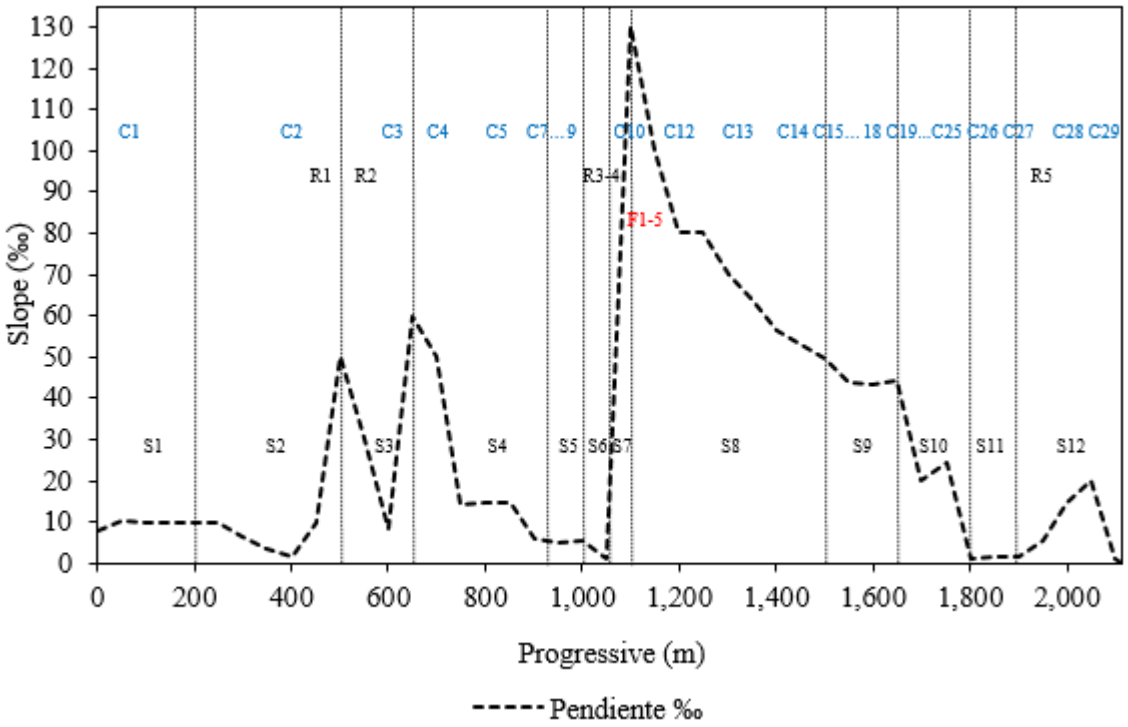

Figure 4: Variation of the slope (‰) of the channel

Depth Response

The depth response was obtained from the lowest vertical distance of the channel section to the central axis of the free flow surface. The results of the depth are observed in Figure 6 and Figure 7. The variability of the depth stands out according to the local characteristics found in each section, whether they are: curves, steep slope channel and drops. Additionally, the calculation of the critical depth was carried out, whose value is constant, because the value of the critical depth is associated with the geometry and the inlet flow of the channel [11-15].

The depth in the sections with curves produces a non-uniform effect at the point of the free surface, that is, the greatest amount of water mass tends to incline on the external or furthest side of the channel. Consequently, the depth grows in said area, and for the inner or closest side the depth decreases. As seen in Figure 5.

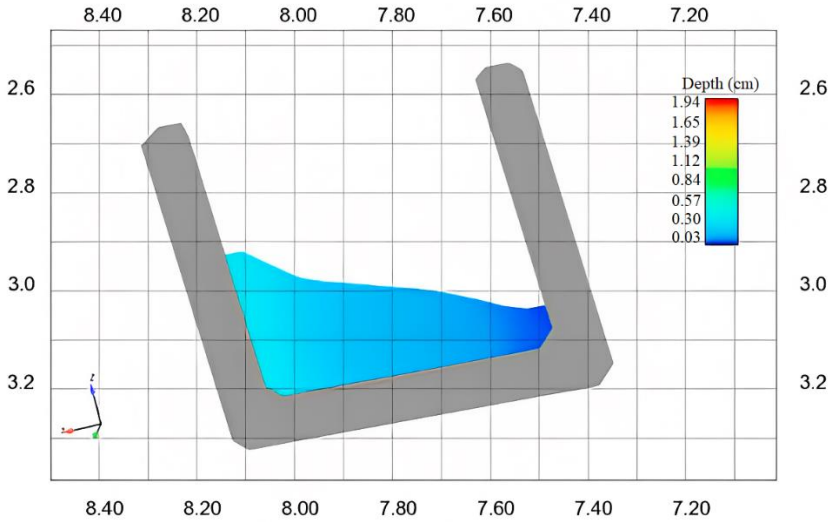

Figure 5: Graph in cut of the depth in curve

The depth decreases in the sections that contain steep slopes. Likewise, it was identified that the effect of energy dissipation is controlled, due to the short lengths of those local characteristics. Finally, the sections that have drops produce a linear decrease with respect to the calculated stays.

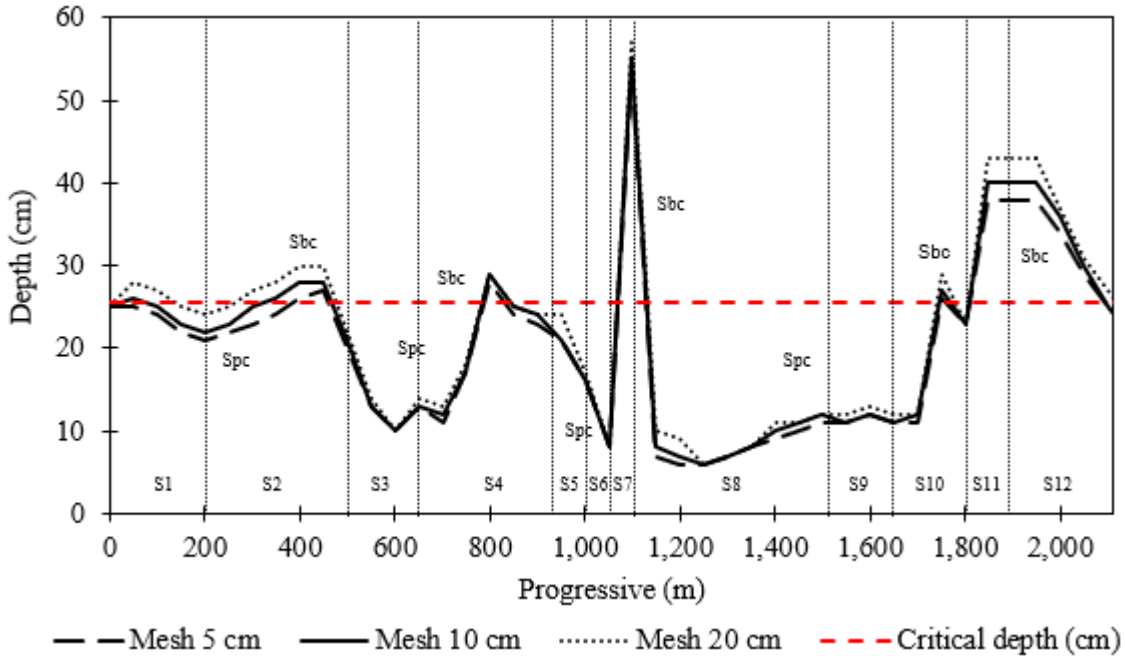

Figure 6: Open channel depth in Iber model

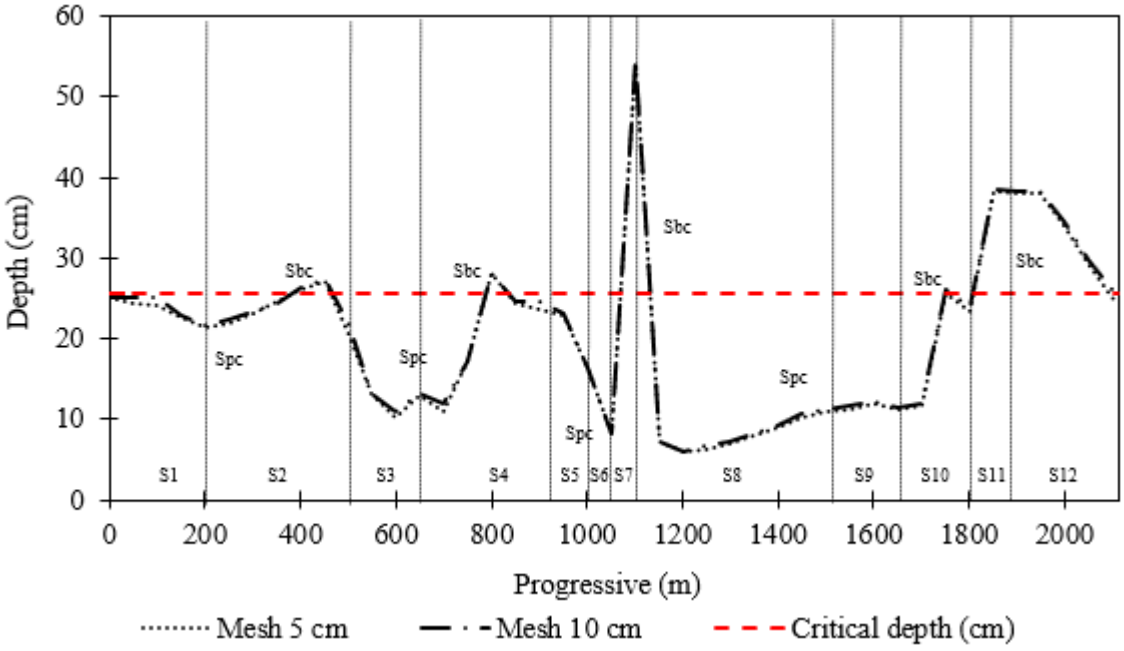

Figure 7: Open channel depth in Flow 3D model

Velocity Response

The velocity response was obtained at the same points as depth results, as shown in Figure 9 and Figure 10, the change in velocity is represented according to the particularities found. Additionally, the calculation of the critical velocity was carried out, whose value is constant throughout the channel, because it is related to the critical depth [16,17].

The volume of water tends to slope towards the outer wall of the greater radius of curvature; as seen in Figure 8. The velocity that prevails in the curves is mostly above or close to the critical velocity.

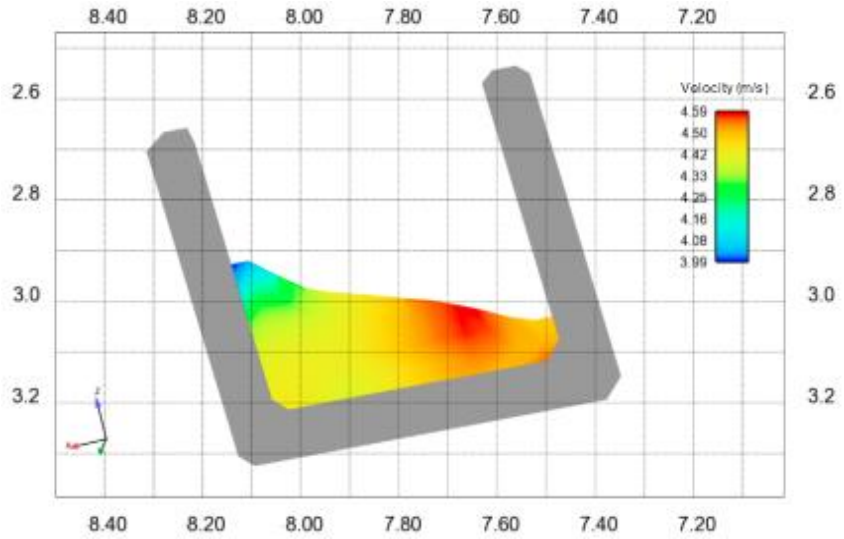

Figure 8: Graph in cut of the velocity in curve

The steep slope channel produces significant velocity increase. On the other hand, the drops generate linear growth of the velocities found. However, the channel has a low flow rate, variable material, and heights of vertical and horizontal drops of less than one meter; therefore, the frictional forces produced by the impact of the flow against the channel walls do not create problems [18-20].

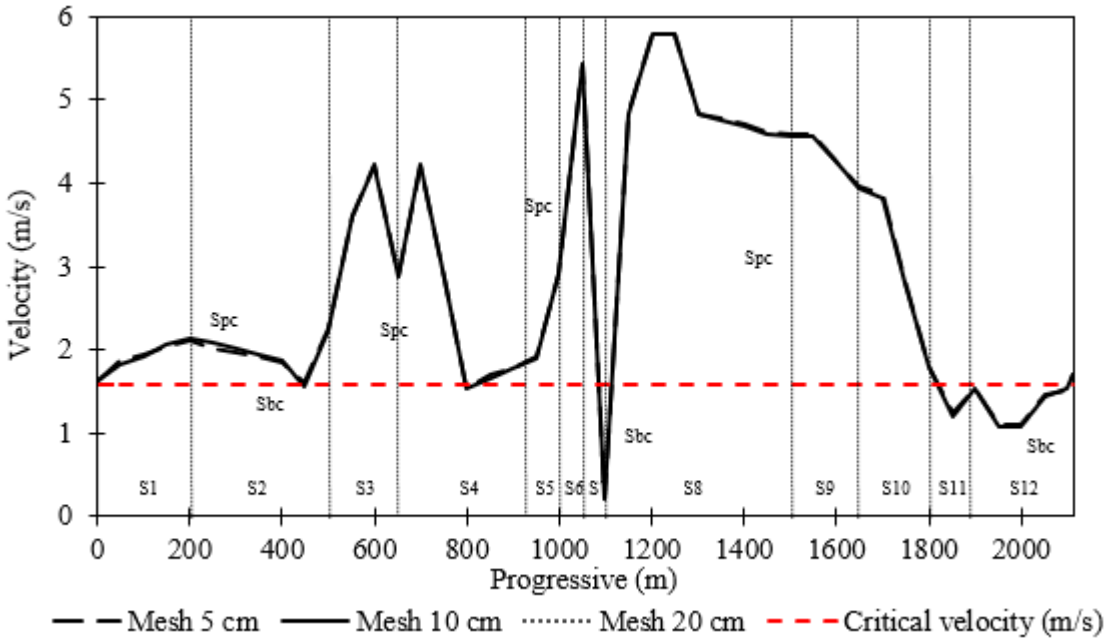

Figure 9: Open channel velocity in Iber model

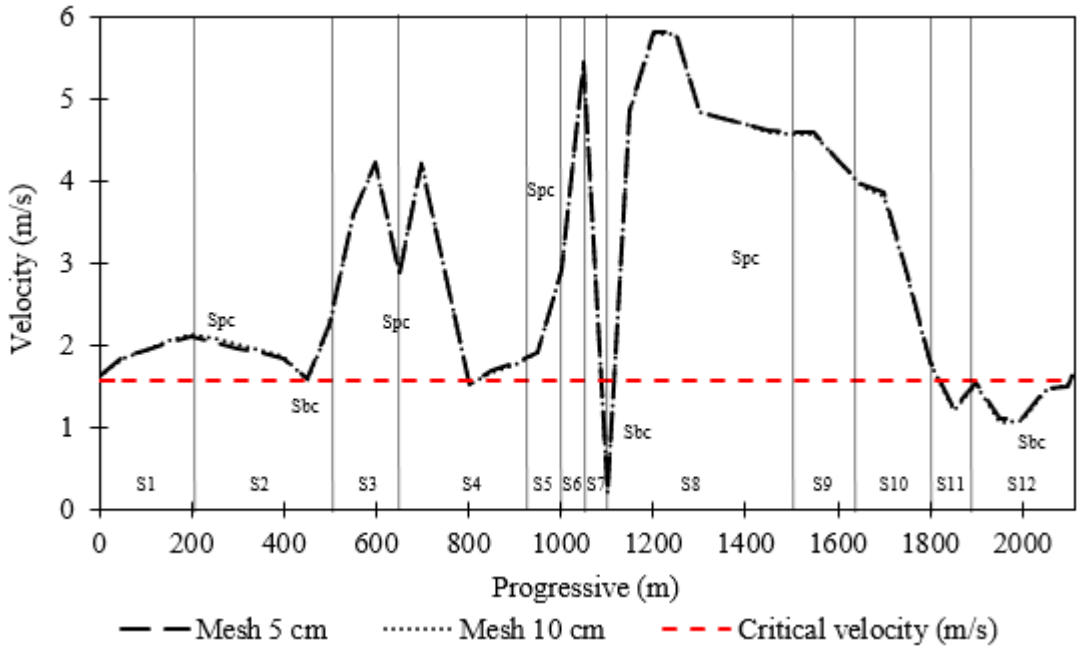

Figure 10: Open channel velocity in Flow 3D model

Type of Regime

The type of regime is determined by the analysis of the Froude number (FR) and the criteria of critical depth and critical velocity. The Iber and Flow 3D models obtained the value of the Froude number for each simulated mesh, and it was corroborated with the general formula. Then, the estimation of the open channel regime mostly composes a supercritical flow regime, as represented in the previous figures of the response of the depth and velocity.

Flow-to-Mesh Ratio

The flow - mesh relationship in the 2D model is correlated in time and space of the flow, evidencing the particularities found in the channel. In addition, the meshes with the greatest acceptability in relation to flow are 5 cm and 10 cm, while those of 20 cm do not differ so much from reality, but events such as steep slope channels and drops, they generated differences in the response. As seen in Figure 11.

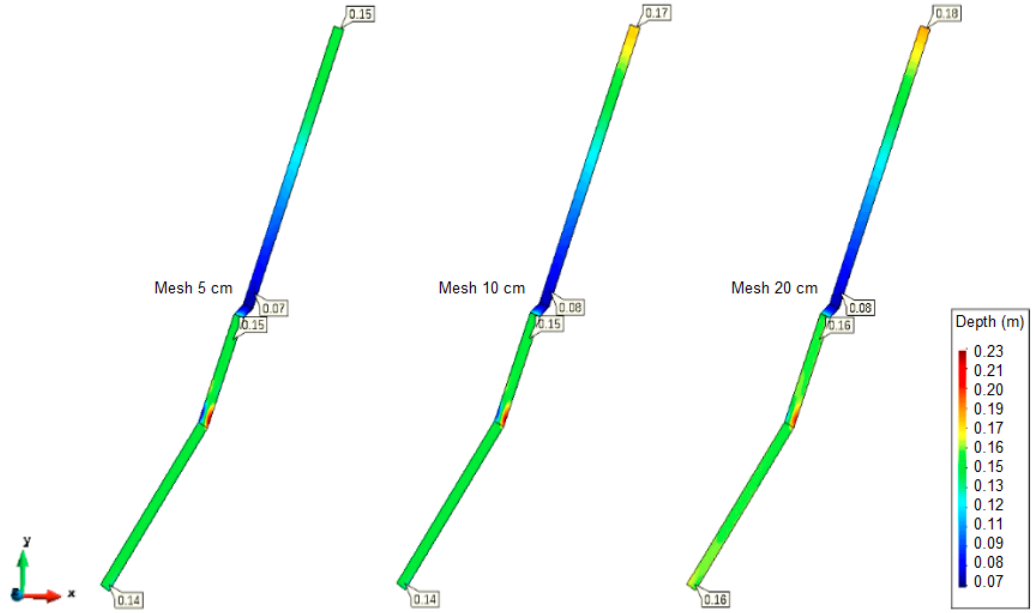

Figure 11: Iber flow – mesh ratio

In the 3D model, the flow-mesh relationship characterizes the geometry through the graphic quality of the channel faces, which are based on the computational cells that make up the 3 planes of each mesh. The rendering of the 5 cm mesh was quite acceptable, as can be seen in Figure 12. The 10 cm mesh suffered complications, particularly in local phenomena, so it was decided to place 7 cm meshes in a non-representative way to cover the area. Finally, the 20 cm mesh represented a problem without solution, in other words, the geometry of the channel could not be interpreted in the model.

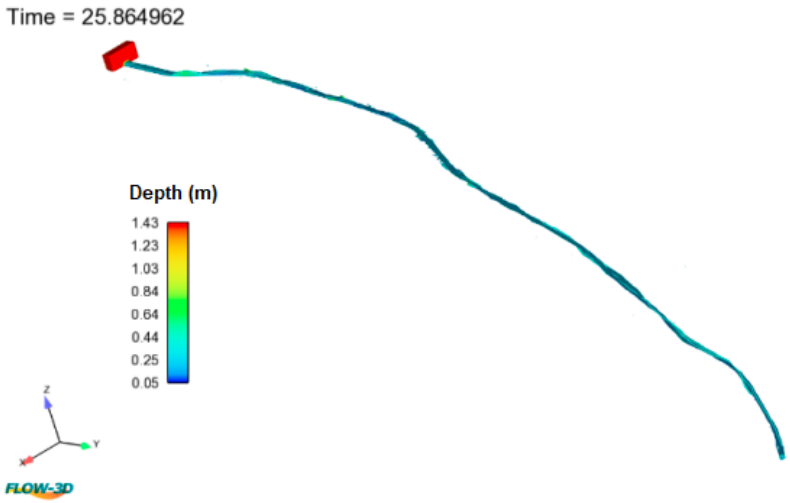

Figure 12: Flow 3D flow – mesh ratio

Local Aspects of Representative Sections

The local aspects of the sections are those that generate suggestive phenomena, as observed in Figure 13, such as hydraulic jumps, rating curve in rapidly varied and gradually varied flows, respectively; Regardless of the mesh size, the trend that makes up the results of the depth and velocity in 2D and 3D models is similar [21,22]. That is, there are no major differences when using a 5 cm and 10 cm mesh, however, for the 20 cm mesh there is some variety. The most representative section is section 7 since the other sections generate controllable or imperceptible local phenomena.

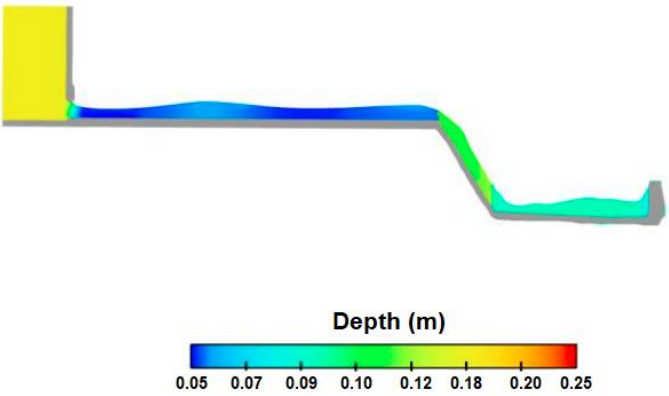

Figure 13: Longitudinal section of suggestive phenomenon in 3D

In section 7, between survey stations 1+050 m and 1+100 m, the hydraulic jump length was calculated using the Sechin method. The Iber model provides the value of the largest conjugate depth (y2 = 0.37 m), which allows determining the hydraulic jump length resulting in 0.95 m. It can be characterized as a weak typology, being a controllable jump that presents good behavior, since the action and position of the flow undulations are not so variable. On the other hand, for the Flow 3D model, the jump length is 1.00 m, contributing the same characteristics of the previous model.

Then, in that section, a transition of depth and velocity is generated, causing the characteristic phenomenon of the rating curve produced by the conditions of the longitudinal profile that represents the free surface, because it changes abruptly [23-27]. That is why the direct method by sections was used, the proportion of distance in each section (Δx) every 10 m of the control section and the total

length of the rating curve (L), giving as the result is a length value of 47.75 m for Iber and 47.93 m for Flow 3D.

Figure 14 shows the theoretical value of the hydraulic jump length of section 7 in Iber. Where an increase in depth is observed, due to the local slope reaching up to 17 cm in survey 1+051. In the following progressives, the hydraulic jump of 0.95 m weak type is produced, then a rating curve of 47.75 m is appreciated. Adding the local phenomena, 49.75 m is obtained, then according to the progressive analyzed (1+050 – 1+100) of 50 m; an error of 0.50% is obtained between the calculated value and the theoretical value.

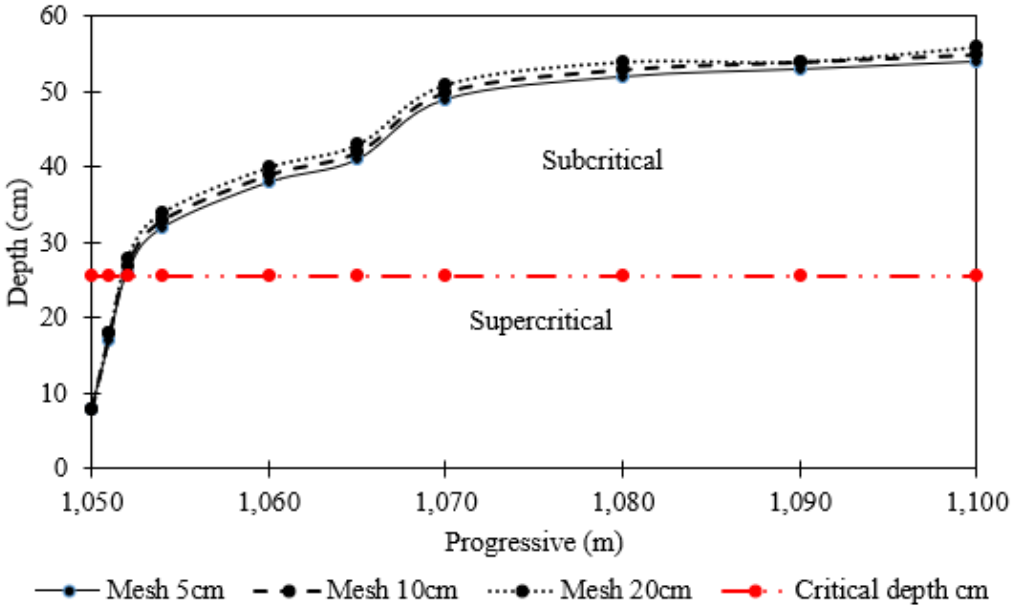

Figure 14: Depth of section 7 of the channel in Iber

Additionally, Figure 15 also shows the theoretical value of the hydraulic jump length of section 7 in Flow 3D model. In the same surveys previously analyzed, the hydraulic jump is produced, obtaining a jump length of 1.00 m. This can be classified as a weak jump, to then obtain a rating curve of 47.93 m, adding the local phenomena, 49.93 m is obtained, finally according to the progressive analysis (1+050 - 1+100) of 50 m.

Then, an error of 0.10% is obtained, between the calculated value and the theoretical (real) value, being within an acceptable criterion for purposes of hydraulic analysis of the rating curve.

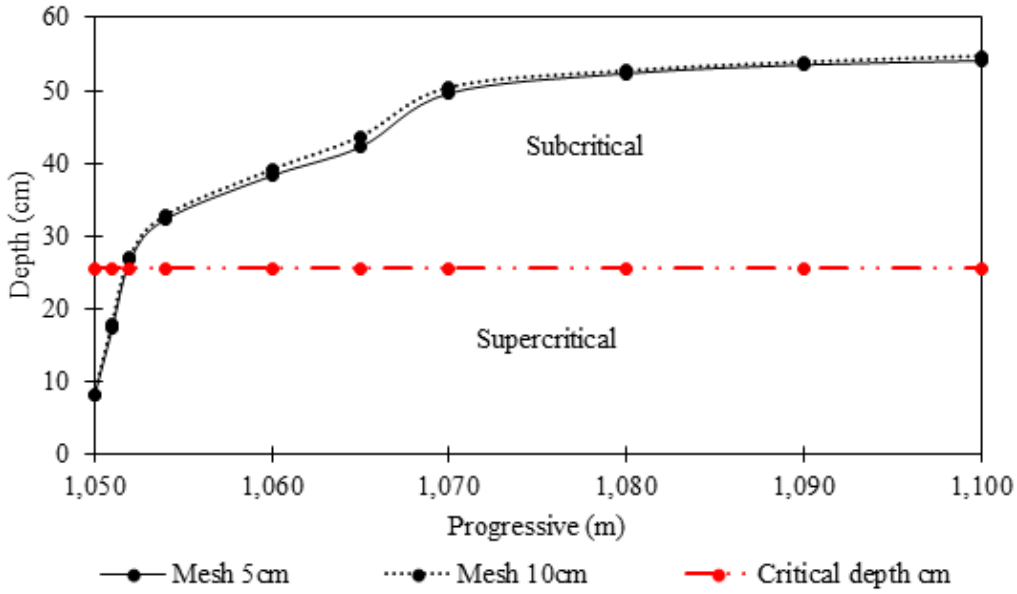

Figure 15: Depth of section 7 of the channel in Flow 3D

Computational Time Analysis

The simulation time using 2D and 3D models is longer with the use of smaller meshes (5 cm and 10 cm). Because, in each section, more computational cells enter to be calculated in the modelling solver and, therefore, the computational domain increases.

In addition, it is observed that in the short or medium sections the time increases in the presence of steep slope channels. In the case of section 8 with the use of the three study meshes (5cm, 10 cm and 20 cm) it was the one that took more simulation time. That is, because it is the only section that has drops.

On the other hand, it is evident that the curves do not have much influence on the increase in time, at least not as much as the number of steep slope channels, but the presence of drops does significantly influence the time delayed by each section. In the case of straight sections, the simulation time does not suffer major complications.

Fig 16 represents the accumulated time of each mesh in Iber. If an average simulation time between the two computers is considered, the variation of time from mesh to mesh, with respect to the mesh of 5 cm (longer time) it follows that the mesh of 10 cm represents 35.6% and the mesh of 20 cm represents 16.0% of the time of the mesh of 5 cm.

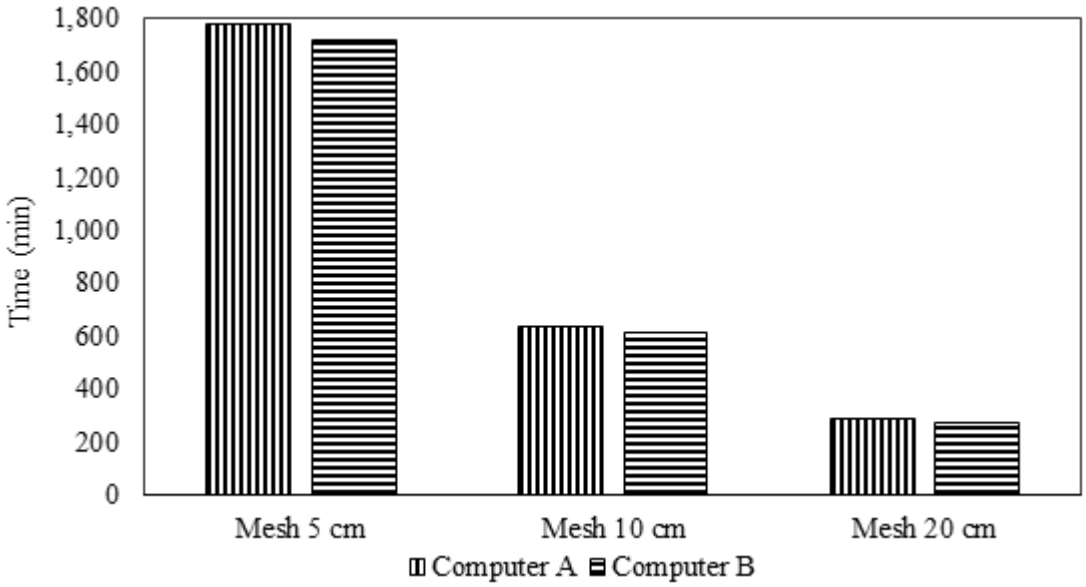

Figure 16: Accumulated simulation time in Iber

The computational time of the Iber model allows for determining two trend curves for the simulation time of each computer, as observed in Figure 17. The model was fitted to a polynomial curve of the second degree, because the variation in time between one computer and another is not large, because the equations are similar, and the graphs are approximate, both resulting in the correlation coefficient equal to 0.955 in the case of computer A and 0.096 in the case of computer B. This indicates that trend lines optimally represent curves.

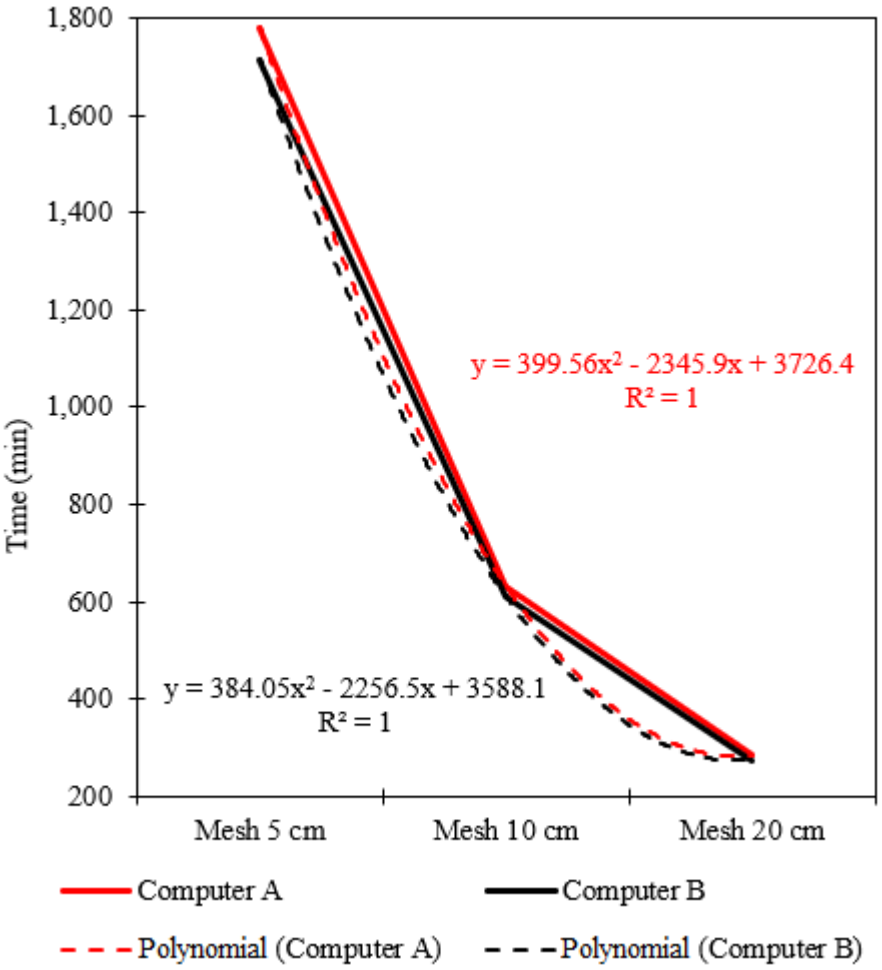

Figure 17: Trend of accumulated time in Iber

Similarly, Figure 18 represents the accumulated time of each mesh in Flow 3D. If an average simulation time between the two computers is considered, the time variation from mesh to mesh; Regarding the 5 cm mesh, it can be deduced that the 10 cm mesh represents 69.60% and the 20 cm mesh represents 5.40% of the time of the 5 cm mesh.

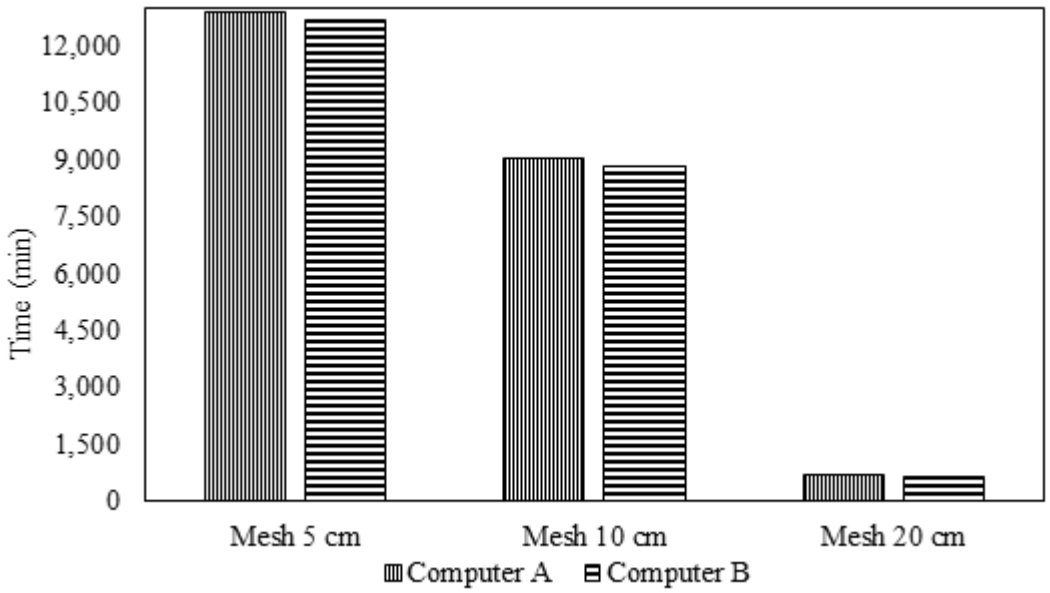

Figure 18: Accumulated simulation time in Flow 3D

Similarly, in the 3D model represented in Figure 19, two second-degree polynomial trend curves are observed for the computational time of each computer, both resulting in the correlation coefficient equal to 0.979 in the case of computer B and 0.978 in the case of computer A.

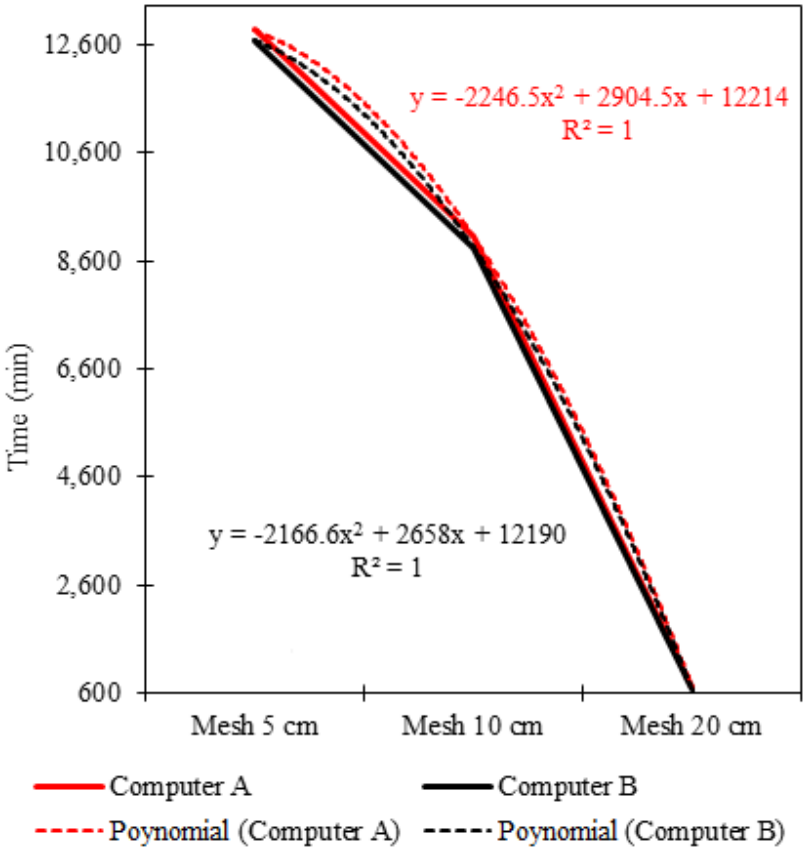

Figure 19: Trend of accumulated time in Flow 3D

The comparative analysis between the two-dimensional and three-dimensional computing time between the Iber and Flow 3D software respectively, was made based on the average of the times obtained by computer A and B, as shown in Table 5.

Average time (min)		
Mesh size	**Iber**	**Flow 3D**
Mesh 5 cm	1747	12776
Mesh 10 cm	622	8938
Mesh 20 cm	279	686

Table 5: Average computational time of Iber and Flow 3D

In the bar graph, Figure 20 shows in the first mesh (5 cm) a considerable variation of time between Iber and Flow 3D, because the simulation time in two-dimensional represents 13.67% of the time of the three-dimensional analysis.

In the second mesh (10 cm) there is also a large time difference between both programs, the total time of Iber represents 6.95% of the time in Flow 3D. However, graphically in the 20 cm mesh there is no great variation in time between both analyses, but in terms of percentage the Iber time is 40.74% of the time in Flow 3D.

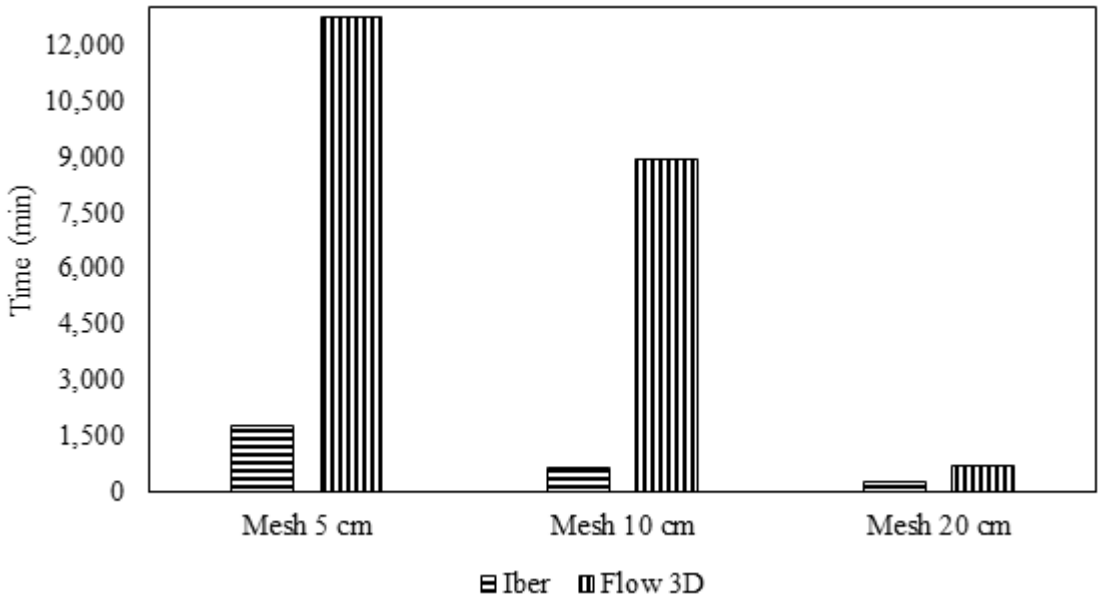

Figure 20: Iber and Flow 3D simulation time

The simulation time with the use of Iber varies according to the mesh size used. For example, the simulation time of the 20 cm mesh is 16.00%, depending on the 5 cm mesh and the simulation time of the 10 cm mesh is 35.60%. Now, the trend line for this software is second-degree polynomial and pretty much fits the curve. Whereas the correlation coefficient being positive indicates that the X and Y axis are directly related.

On the contrary, in the results obtained in Flow 3D the time of variation from mesh to mesh is wider. The time obtained in the 20 cm mesh is 5.37% compared to the 5 cm mesh, in addition the time obtained in the 10 cm mesh is 69.95% compared to the 5cm mesh. Similarly, the trend line for this software is second-degree polynomial and does not fit as much as in Iber. Whereas the correlation coefficient being positive indicates that the X and Y axis are directly related.

When comparing both 2D and 3D models, see Figure 21, the two trend curves for the simulation time of each program were determined, in the same way the polynomial curve of second degree is better approximated to the graphs, resulting in the correlation coefficient equal to 0.95 for Iber and 0.098 in the case of Flow 3D, this means that it has a better representation of the data to the fitted regression line.

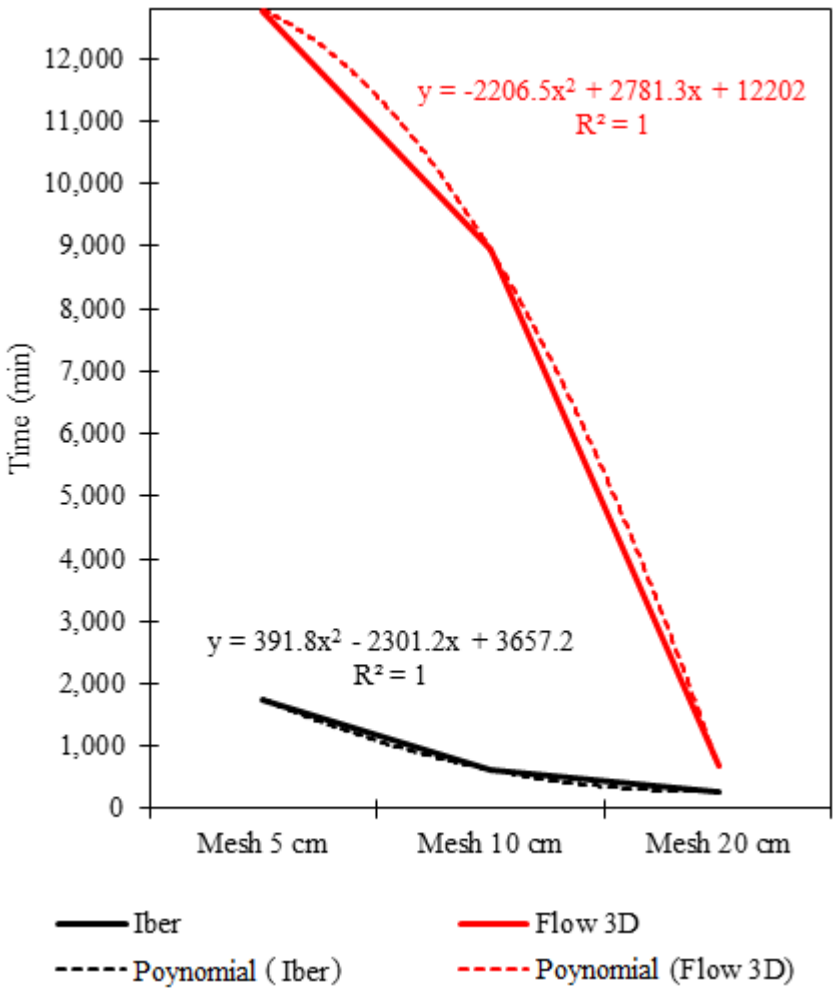

Figure 21: Iber and Flow 3D computational time trend

The accuracy was determined by the relative error for each control point of each section, in relation to the value of the stay found in the field (Zita, 2018). It follows from Figure 22 and Figure 23 that in Iber the most accurate mesh is 5 cm, because the average relative error value is 1.10 %. Similarly, for Flow 3D the most accurate meshing is also 5 cm with a value of 1.77%. When comparing both programs, it follows that the most accurate is from the Iber software, with a difference between them of 0.67%.

Accuracy was determined by measuring the calculated value of the mean and standard deviation for each mesh. Because, the less dispersion, the greater the precision of Figure 22 and Figure 23, it is inferred that Iber has greater precision. This is because it has a lower standard deviation value (Zita, 2018) in the 5 cm mesh, with a value of 10.45. On the other hand, in Flow 3D the mesh with greater precision was also 5 cm. Therefore, when comparing both programs, the one that has the most accuracy is the Flow 3D with a deviation of 10.44. However, the difference between the two of 0.009 is considered quite short.

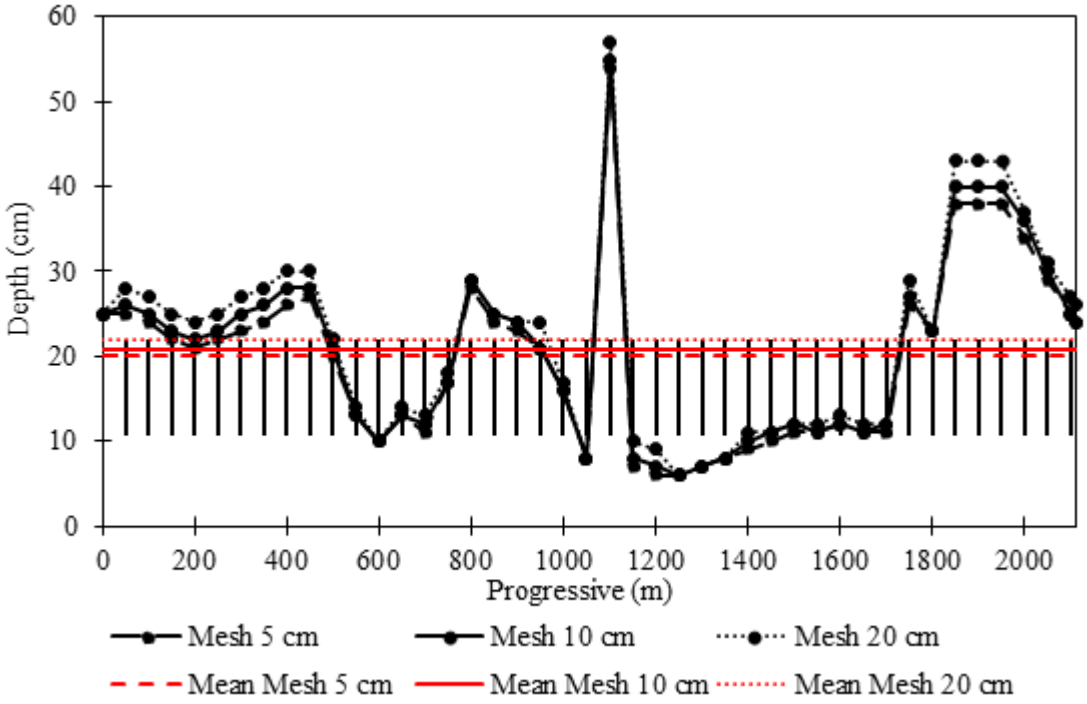

Figure 22: Accuracy and precision in Iber

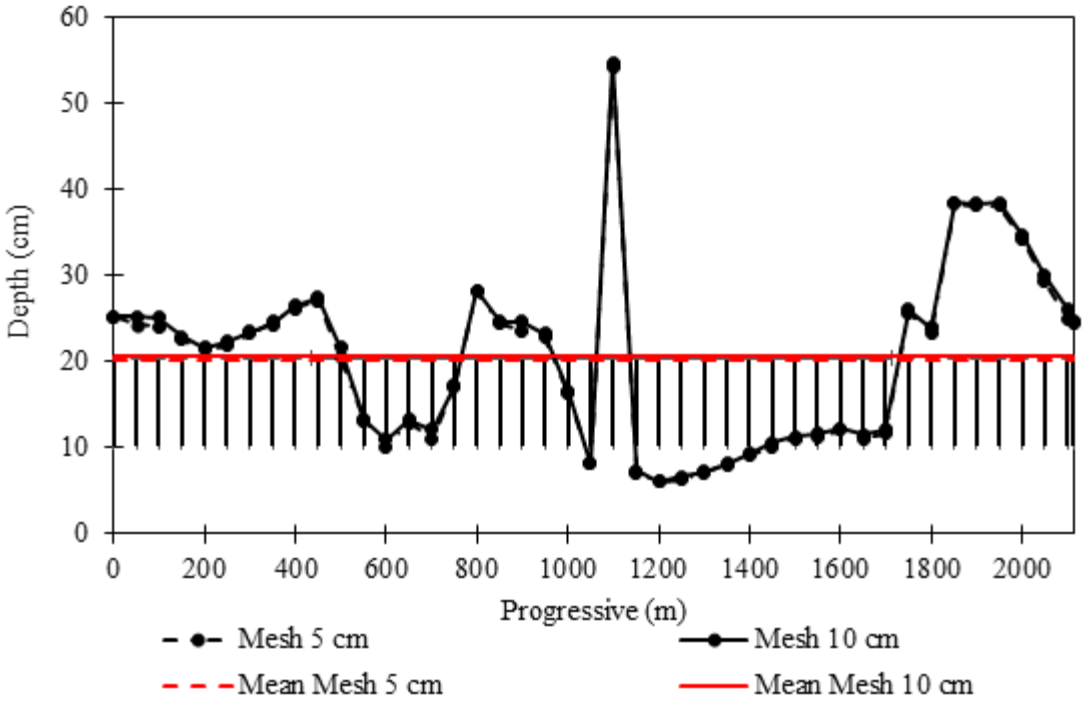

Figure 23: Accuracy and precision in Flow 3D

4. Conclusions

The 2D and 3D models implemented in Iber and Flow 3D software, for the rural open channel of the district of Pocsi, in Arequipa, allowed to optimize the hydraulic simulation correlating the measurement of the computational time with the level of accuracy and precision of the size of the Mesh. considering the following:

- The accuracy of Iber and Flow 3D was presented in the

5 cm mesh with a relative error of 1.10% and 1.77%, respectively. In this way obtaining a difference between the two of 0.67%. On the other hand, each software presents the highest precision in the 5 cm mesh, with a standard deviation of 10.45 in Iber and 10.44 in Flow 3D; When comparing both models, the one with the highest accuracy is Iber and the greatest precision is shown in Flow 3D.

- The Iber 2D model represents a synchronization of the meshes with the traced free surface, regardless of the flow direction; it also presents shorter simulation times. On the other hand, the Flow 3D model applied to open channels requires a lot of computational time, however, for local phenomena it represents greater detail sensitivity.
- The computational time and mesh size directly affected the hydraulic simulation of 2D and 3D models, implemented in Iber and Flow 3D software, respectively, since both programs are governed by computational fluid dynamics, collecting as results:
- The post-process computational time was greater in three-dimensional simulation, since it took around 373 hours, while two-dimensional simulation took approximately 44 hours. That is, a variation of 329 hours, in terms of percentage, Iber took 11.80% of the total time of Flow 3D.
- Regarding the mesh, the 5 cm mesh turned out to be the one with the highest sensitivity of results, due to the adjustment of the computational cells in the geometry of the channel, however, the computational domain grows, which means that the file requires more memory, storage, and power hardware capacity. On the other hand, the computational time of Iber, with a 5 cm mesh, took 13.67% compared to Flow 3D; As for the 10 cm mesh, it took 6.95% of the time in Flow 3D and the 20 cm mesh took 40.74% of the time in Flow 3D.
- In Flow 3D software, the 10 cm mesh presented rendering problems in the channel geometry, specifically in the sections with long lengths, drops and long curves. In these areas, the meshing had to be reduced, specifically with a 7 cm mesh, representing 4.81% of the total length of the channel to obtain considerable results. In addition, with the 20 cm mesh the simulation was not possible, due to the number of gaps that occur in the rendering prior to the model, so it was not possible to obtain results.
- The results obtained in the hydraulic simulations of 2D and 3D models, presented important differences according to the level of sensitivity of each software, where an optimal model of reduced computational time and an adequate mesh size were found, determining the following:
- The Iber model, with meshes of 5 cm and 10 cm, have error percentages of 1.10% and 3.86% respectively, in terms of the depth calculated and the ones obtained in the field inspection. On the other hand, the results of the 3D model with 5 cm and 10 cm mesh are also within the permissible range of error, with a value of 1.77% and 3.09% correspondingly [28-35].
- The model optimized for the channel under study, regarding the mesh size and computational time for Iber 2D is the 5 cm mesh, and for Flow 3D it is the 10 cm mesh. This is because both present a greater quality of results and shorter hydraulic modelling period for each software.

Ethical Approval

This article does not include third-party or animal research by any of the authors.

Consent to Participate

Informed consent was obtained from all participants individually for publication.

Consent to Publish

Informed consent was obtained from all participants individually involved in the study.

Authors Contributions

All authors involved contributed to the methodology, 2D and 3D modelling, statistical analysis, research, resources, and writing of the original draft. Furthermore, all authors have read and accepted the published version of this manuscript.

Funding

There is no source of funding.

Competing Interests

There are no conflicts of interest on the part of the authors.

Availability of Data and Materials

On reasonable request.

References

1. Urquizo, L. (2021). Technical file of the Improvement of the irrigation system of the canal between the reservoir of Huichuna to the sector of Choja of the District of Pocsi - province of Arequipa - department of Arequipa. Pocsi District Municipality.
2. Moya, R. and Álvarez, W. (2018). Hydraulic modelling of an urban canal in the city of Bogotá, case study: Rio Negro channel. [Undergraduate thesis, Catholic University of Colombia].
3. Flumen. (2014). Hydraulic reference manual. Center for studies and experimentation of public works. Water and environmental engineering group. Ministry of Environment and Rural Marine Affairs of Spain.
4. Vargas, J. (2019). Comparative study of the Hec-Ras, Iber and Flow 3D softwares in studying flow characteristics across a dynamic meander in Colombia. Research Gate. Laval (Greater Montreal).
5. Andrade, A. Schulz, H. de Melo R. (2017). Computational Methods in Hydraulics. Editor of the Federal University of Bahia.
6. Bendezu, J. (2017). Evaluation of hydraulic phenomena and two-dimensional modelling with Iber in variable slope channel. [Undergraduate thesis, Universidad Nacional de San Cristóbal de Huamanga].
7. Bohórquez, C. (2020). Numerical modelling (CDF) of the upper and lower combined flow in a flat gate with the Flow 3D program. [Master's Thesis, National Polytechnic School].

8. Casa, E. et al. (2018). Numerical modelling of the grazing flow in a rapid step applying computational fluid dynamics (CFD) using Flow-3D. Polytechnic Review, Vol. 41 (No. 2).
9. Castro, P. and García, C. (2021). Two-dimensional modelling proposal for the estimation of mesh size and computational time in channels wide of 100 meters using Iber 2.5.2. and HEC-RAS 5.0.7. [Undergraduate thesis, Universidad Private Antenor Orrego].
10. Cengel, Y. and Cimbala, J. (2006). Fluid mechanics. McGrawHill.
11. Chow, V. T. (1994). Hydraulics of open channels. McGraw-Hill.
12. Díaz, V.and Urbano J. (2020). Comparative study of an open conduction system and a closed conduit of the Mochalito - Poroto - Trujillo - La Libertad channel. [Undergraduate thesis, University Cesar Vallejo].
13. Fernández, C., León, A. and Martínez, P. (2018). Influence of the estimation method on the Manning coefficient for natural channels. Hydraulic and Environmental Engineering, Vol. XXXIX, (pp. 17-81).
14. Fernández, J. (2012). Numerical techniques in fluid engineering. Introduction to computational fluid dynamics (CFD) by the finite volume method. Editorial Reveté.
15. García, N. (2016). Channel hydraulics Basic principles. Mexican Institute of Water Technology.
16. Guncay, K. (2017). Study of the hydraulic performance of the multipurpose channel of the LH&DF fluid dynamics and hydraulics laboratory of the Balzay campus. [Undergraduate thesis, University of Cuenca].
17. Hurtado, J. (2000). Methodology of Holistic Research. Sypal Foundation.
18. Lacasta, A. (2012). Preprocess static subdomain decomposition in practical cases of 2D unsteady hydraulic simulation. Preprint submitted to Computers & Fluids.
19. López, A. (2015). Numerical resolution of the Navier-Stokes equations. [Undergraduate thesis, University of Cantabria].
20. Manay, J. (2019). Modelling of free surface flow in the Taymi channel km 33+000 to km 38+000, Lambayeque. [Undergraduate thesis, Universidad Señor de Sipán].
21. Martinez, E. (2013). 1D, 2D and 3D modelling of a curved section of the PAC-UPC laboratory channel. [Master's thesis, Polytechnic University of Catalonia].
22. Maselhe, G. (2012). Numerical modelling of hydrodynamics and sediment transport in lower Mississippi at a proposed delta building diversion. Journal of Hydrology.
23. Moukalled, F., Mangani, L., y Darwish, N. (2016). The Infinite Volume Method in Computational Fluid Dinamics. Publishing AG Switzerland.
24. Ñaupas, H., et al (2014). Research methodology. Editions of the U.
25. Patiño, D and Vintimilla, D. (2015). Analysis of the behavior of the flow through a fan landfill and its subsequent dissipating bowl using a three-dimensional flow mathematical model. [Undergraduate thesis, University of Cuenca].
26. Potter, M. Wiggert, D. (2015). Fluid mechanics. Editorial Engineering sciences.
27. Quishpe, D. (2021). Manual of virtual laboratory practices, applying numerical modelling (CFD) for use in the subjects of fluid mechanics and applied hydraulics. [Undergraduate thesis, Universidad Politécnica Salesiana headquarters Quito].
28. Recasens, J. (2014). Three-dimensional modelling of the inlet flow in a sink 711-TESCA-6388. [Thesis, Polytechnic University of Catalonia].
29. Ring, P. (2021). Class 14 Basic Hydraulics. Fundamental equations.
30. Salamea, T. (2015). Hydrodynamic two-dimensional modelling of sediment flow and transport through the Calabí River and hydraulic works. [Undergraduate thesis, University of Cuenca].
31. Strezt, C. (2021). Hydraulic modelling to maximum avenue of the spillway of too many of the dam of Condoroma – Arequipa. [Undergraduate thesis, Catholic University of Santa Maria].
32. Torres, J. (2017). Hydraulic Design and Modelling in HEC-RAS of the Concrete Canal and Works of Art of the Carpenter Project – Section Km 0+000 to Km 5+000. [Undergraduate thesis, Peruvian University of Applied Sciences].
33. Villon, M (1985). Channel hydraulics. Editorial Horizonte Latin-American.
34. Willis, E. (2015). Optimization of the hydraulic design of the Miraflores project using the Telemac-2D numerical model. [Undergraduate thesis, University of Piura, Piura, Peru].
35. Zita, A. (2018). (July 25, 2022). Accuracy and precision. Theydiffer.